Journal of ELECTRONIC MATERIALS, Vol. 40, No. 5, 2011
DOI: 10.1007/s11664-010-1463-2

Enhanced Thermoelectric Properties Obtained by Compositional Optimization in *p*-Type $Bi_xSb_{2-x}Te_3$ Fabricated by Mechanical Alloying and Spark Plasma Sintering

CHEN CHEN,[1,2] DA-WEI LIU,[1] BO-PING ZHANG,[2] and JING-FENG LI[1,3]

1.—State Key Laboratory of New Ceramics and Fine Processing, Department of Materials Science and Engineering, Tsinghua University, Beijing 100084, China. 2.—Beijing Key Laboratory of New Energy Materials and Technology, School of Materials Science and Engineering, University of Science and Technology Beijing, Beijing 100083, China. 3.—e-mail: jingfeng@mail.tsinghua.edu.cn

$Bi_xSb_{2-x}Te_3$ bulk alloys are known as the best *p*-type thermoelectric materials near room temperature. In this work, single-phase $Bi_xSb_{2-x}Te_3$ (x = 0.2, 0.25, 0.3, 0.34, 0.38, 0.42, 0.46, and 0.5) alloys were prepared by spark plasma sintering (SPS) using mechanical alloying (MA)-derived powders. A small amount (0.1 vol.%) of SiC nanoparticles was added to improve the mechanical properties and to reduce the thermal conductivity of the alloys. The electrical resistivity decreases significantly with increasing ratio of Sb to Bi in spite of the weaker decreasing trend in Seebeck coefficient, whereby the power factor at 323 K reaches 3.14×10^{-3} W/mK^2 for a sample with x = 0.3, obviously higher than that at x = 0.5 (2.27×10^{-3} W/mK^2), a composition commonly used for ingots. Higher thermal conductivities at low temperatures are obtained at the compositions with lower x values, but they tend to decrease with temperature. As a result, higher ZT values are obtained for $Bi_{0.3}Sb_{1.7}Te_3$, with a maximum ZT value of 1.23 at 423 K, about twice the ZT value (about 0.6) of $Bi_{0.5}Sb_{1.5}Te_3$ at the same temperature.

Key words: $Bi_xSb_{2-x}Te_3$, spark plasma sintering, mechanical alloying

INTRODUCTION

Thermoelectric (TE) devices are capable of the direct conversion of electricity and thermal energy for cooling or heating, which can be used to recover waste heat for conversion into electrical power. Therefore, the potential applications of TE devices in waste heat recovery, air conditioning, and refrigeration have attracted increasing interest.[1–5] Bi_2Te_3-based alloys such as $Bi_xSb_{2-x}Te_3$ (*p*-type) are some of the most important thermoelectric materials for use near room temperature and have been widely used in commercial thermoelectric materials. $Bi_xSb_{2-x}Te_3$ has remarkable crystallographic anisotropy that originates from the rhombohedral structure composed of five atomic layers [-$Te^{(1)}$-Sb-$Te^{(2)}$-Bi-$Te^{(1)}$-], stacked by van der Waals interactions along the *c*-axis.[5,6] Conventionally, zone melting (ZM), Bridgman, and Czochralski methods are often used to prepare $Bi_xSb_{2-x}Te_3$ ingots with excellent TE properties.[7] However, it is difficult to fabricate TE modules from such ingots, because of their poor mechanical properties. In recent years, many methods such as shear extrusion, melt spinning, hydrothermal synthesis, and hot pressing have been applied to prepare polycrystalline $Bi_xSb_{2-x}Te_3$ alloys.[8–11]

The composition of $Bi_{0.5}Sb_{1.5}Te_3$ was historically thought to have the optimized carrier density, and it has been used for more than 50 years. As many new methods have been used to synthesize Bi_2Te_3-based alloys, the optimal composition of $Bi_xSb_{2-x}Te_3$ has probably deviated from $Bi_{0.5}Sb_{1.5}Te_3$. The origin of charge carriers in *p*-type $Bi_xSb_{2-x}Te_3$ is related to the antisite defects (Sb_{Te} or Bi_{Te}) where Sb or Bi atoms occupy Te sites.[7] Hence, it is possible to get an optimized carrier density for the best electrical properties by changing the Sb-to-Bi ratio. In this study, $Bi_xSb_{2-x}Te_3$ (x = 0.2, 0.25, 0.3, 0.34, 0.38,

(Received August 18, 2010; accepted November 23, 2010; published online December 29, 2010)

0.42, 0.46, and 0.5) alloys were prepared by spark plasma sintering (SPS) using mechanical alloying (MA)-derived powders. The influence of the Sb-to-Bi ratio on carrier density was clarified by investigating the microstructure and thermoelectric properties of the $Bi_xSb_{2-x}Te_3$ alloys.

EXPERIMENTAL PROCEDURES

Commercial high-purity powders of 99.99% Bi (under 100 mesh), 99.99% Te (under 200 mesh), 99.99% Sb (under 200 mesh), and 99% SiC (average diameter ~100 nm) were used as raw materials. Since dispersion of SiC nanoparticles in Bi_2Te_3 can reduce the thermal conductivity and improve the mechanical properties, as found in our previous studies,[12] a small amount (0.1 vol.%) of SiC nanoparticles was dispersed into $Bi_xSb_{2-x}Te_3$ in the present study.

Powders with chemical compositions of $Bi_xSb_{2-x}Te_3$ + 0.1 vol.% SiC (x = 0.2, 0.25, 0.3, 0.34, 0.38, 0.42, 0.46, and 0.5) were prepared after MA at 450 rpm for 3 h in purified argon atmosphere using a planetary ball mill (QM-3SP2, Nanjing University, China). A stainless-steel vessel and balls were used with the weight ratio of balls to powders kept at 20:1. Subsequently, the as-milled powders were sintered under an axial compressive stress of 50 MPa at 673 K in vacuum using a spark plasma sintering (SPS) system (Sumitomo SPS 1050, Japan) as reported elsewhere.[12–14]

Phase structure of the bulk samples was characterized by x-ray diffraction (XRD, Cu K_α, D/Max-2500; Rigaku, Japan). Fractographs of the bulk samples were observed by scanning electron microscopy (SEM, JSM-6460, Japan). The Seebeck coefficient and electrical resistivity were evaluated along the sample section perpendicular to the SPS pressing direction, while the thermal diffusivity was evaluated along the sample section parallel to the SPS pressing direction. The Seebeck coefficient and electrical resistivity were measured using a Seebeck coefficient/electrical resistivity measuring system (ZEM-2; Ulvac-Riko, Japan) under helium atmosphere in the temperature range from 323 K to 473 K. The thermal diffusivity (D) was measured by the laser flash method using a TC-9000 apparatus (Ulvac-Riko, Japan). The specific heat (C_p) was measured by using a thermal analysis apparatus (DSC-60, Shimadzu, Japan). The density (d) of the samples was measured by the Archimedes method. The thermal conductivity (κ) was calculated from the density (d), specific heat (C_p), and thermal diffusivity (D) using the relationship $\kappa = DC_pd$.[5]

RESULTS AND DISCUSSION

Figure 1 shows XRD patterns of sintered bulk samples with compositions of $Bi_xSb_{2-x}Te_3$ + 0.1 vol.% SiC (x = 0.3 and 0.5). All the diffraction peaks of the bulk materials were obtained from the section perpendicular to the pressing direction. The standard diffraction peaks cited for $Bi_{0.5}Sb_{1.5}Te_3$ (PDF#49-1713) are indicated by vertical lines for comparison. Regardless of the different x values, the characteristic peaks of all the sintered bulk materials matched up well with the standard pattern, indicating the formation of single-phase $Bi_xSb_{2-x}Te_3$ compounds. No characteristic peaks of SiC were found in the XRD patterns owing to the low SiC content (0.1 vol.%).

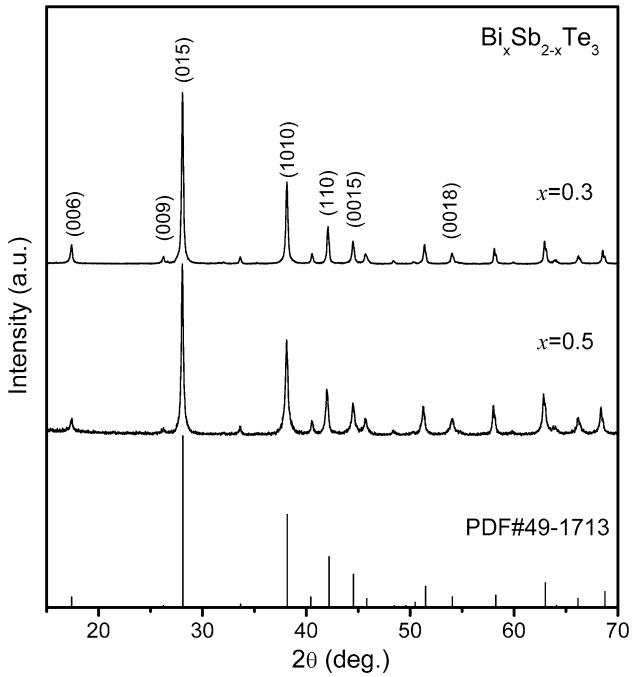

Fig. 1. XRD patterns of sintered bulk $Bi_xSb_{2-x}Te_3$ + 0.1 vol.% SiC (x = 0.3 and 0.5) materials from a section perpendicular to the pressing direction.

Figure 2 presents XRD patterns of $Bi_{0.5}Sb_{1.5}Te_3$ + 0.1 vol.% SiC from sections parallel and perpendicular to the pressing direction for comparison. The relative intensities of (00l) planes from the sections perpendicular to the pressing direction, including (006), (009), (0015), and (0018), are slightly higher than those from the sections parallel to the pressing direction. This indicates that the sections perpendicular to the pressing direction are slightly orientated on (00l) planes. The electrical and thermal conductivities in the c-plane are about four and two times larger than those along the c-axis in Bi_2Te_3-based alloys, respectively.[5] The orientation degree of the (00l) planes, termed F, was calculated by the Lotgering method using the following equations:[6]

$$F = \frac{P - P_0}{1 - P_0}, \tag{1}$$

$$p_0 = \frac{I_0(00l)}{\sum I_0(hkl)}, \tag{2}$$

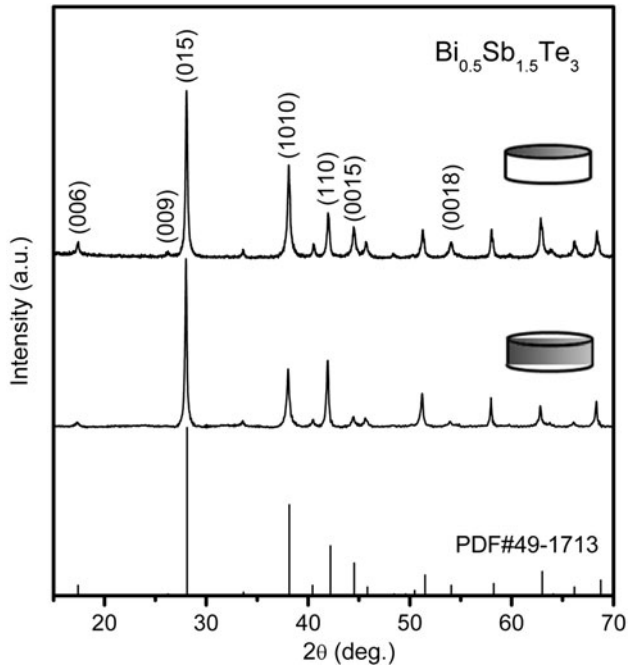

Fig. 2. XRD patterns of sintered bulk $Bi_{0.5}Sb_{1.5}Te_3$ + 0.1 vol.% SiC material from two sections, parallel and perpendicular to the pressing direction, respectively.

$$p = \frac{I(00l)}{\sum I(hkl)}, \tag{3}$$

where P and P_0 are the integrated intensities of all $(00l)$ planes to the integrated intensities of all $(h\ k\ l)$ planes for preferentially and randomly oriented samples, respectively. The F value for $Bi_{0.5}Sb_{1.5}Te_3$ + 0.1 vol.% SiC was about 0.08, which means that the slightly oriented texture can be ignored and the polycrystalline materials prepared by SPS are supposed to be isotropic.

Figure 3 shows SEM fractographs of the sintered $Bi_xSb_{2-x}Te_3$ + 0.1 vol.% SiC (x = 0.3 and 0.5) bulk materials for sections perpendicular and parallel to the pressing direction, respectively. All the samples, regardless of x value, showed lamellar grains with an average size of about 1 μm and dense microstructures with a high relative density of over 94%. Figure 3a, c shows slightly oriented grains in the section perpendicular to the pressing direction as compared with those in the section parallel to the pressing direction (Fig. 3b, d). This result is in good agreement with the XRD pattern in Fig. 2.

Figure 4 shows the temperature dependence of the electrical resistivity for sintered bulk $Bi_xSb_{2-x}Te_3$ + 0.1 vol.% SiC (x = 0.2, 0.25, 0.3, 0.34, 0.38, 0.42,

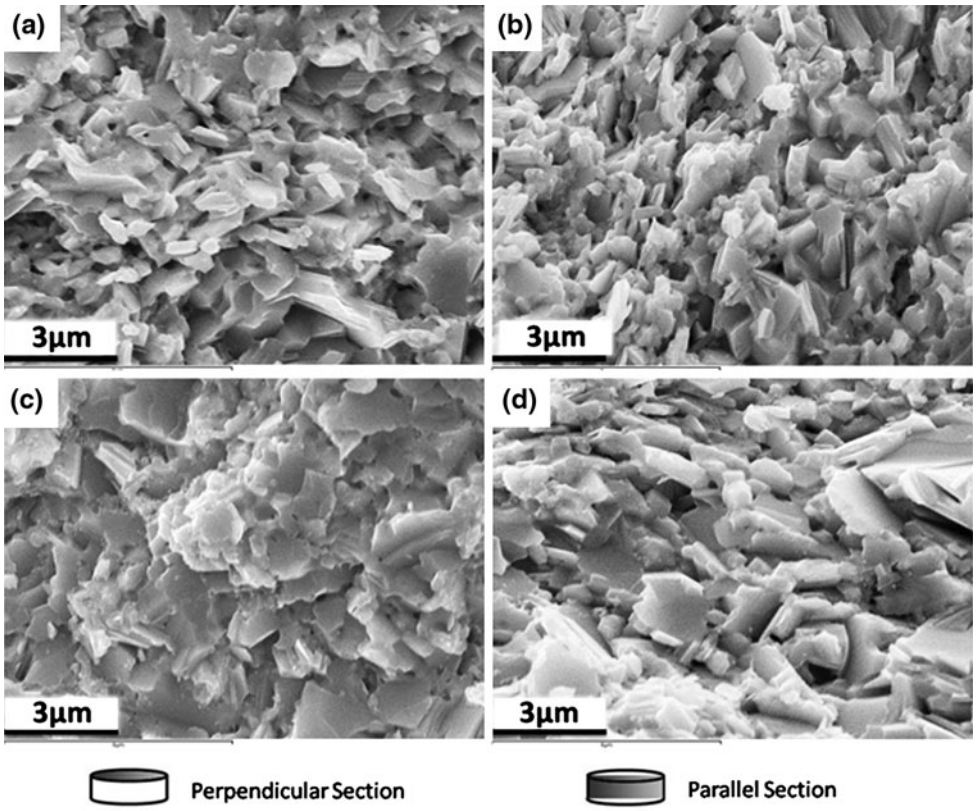

Fig. 3. SEM fractographs of the sections perpendicular (a, c) and parallel (b, d) to the pressing direction for sintered bulk $Bi_xSb_{2-x}Te_3$ + 0.1 vol.% SiC materials with (a, b) x = 0.5, and (c, d) x = 0.3.

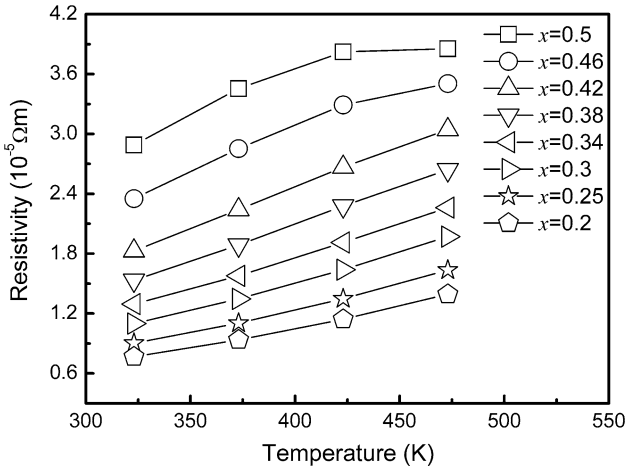

Fig. 4. Electrical resistivity of sintered bulk $Bi_xSb_{2-x}Te_3$ + 0.1 vol.% SiC (x = 0.2, 0.25, 0.3, 0.34, 0.38, 0.42, 0.46, and 0.5) materials as a function of measurement temperature.

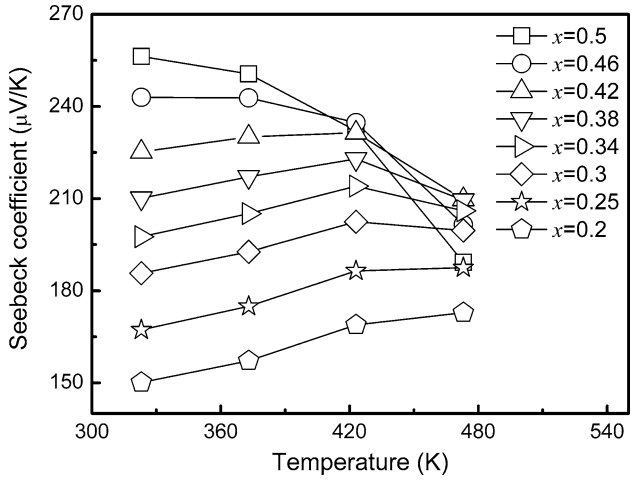

Fig. 5. Seebeck coefficient of sintered bulk $Bi_xSb_{2-x}Te_3$ + 0.1 vol.% SiC (x = 0.2, 0.25, 0.3, 0.34, 0.38, 0.42, 0.46, and 0.5) materials as a function of measurement temperature.

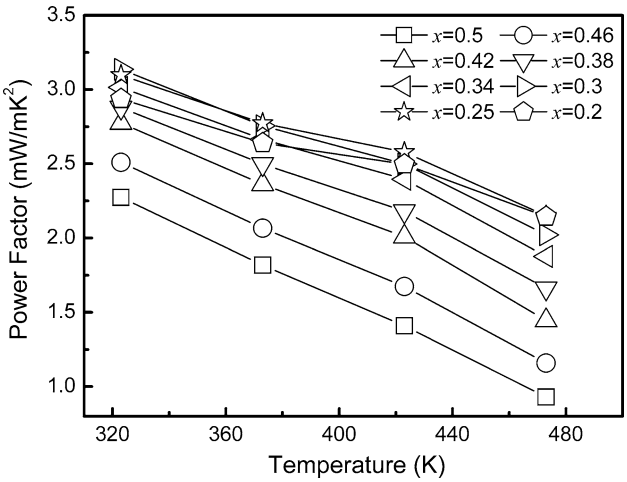

Fig. 6. Power factor of sintered bulk $Bi_xSb_{2-x}Te_3$ + 0.1 vol.% SiC (x = 0.2, 0.25, 0.3, 0.34, 0.38, 0.42, 0.46, and 0.5) materials as a function of measurement temperature.

0.46, and 0.5) materials. The electrical resistivity of all the samples increases with increasing measurement temperature from 323 K to 473 K, indicating metallic conducting behavior. The electrical resistivity of $Bi_{0.5}Sb_{1.5}Te_3$ was about 2.89 × 10^{-5} Ω m at room temperature and decreased with decreasing x value, which is mainly caused by the enhanced carrier density. The minimum electrical resistivity value (7.7 × 10^{-6} Ω m) was obtained at 323 K for $Bi_{0.2}Sb_{1.8}Te_3$. It is well known that the major charge carrier in $Bi_{0.5}Sb_{1.5}Te_3$ is created by antisite defects where Sb atoms occupy Te sites, which can be described as: $Sb_2Te_3 = 2Sb'_{Te} + V^{\cdot\cdot}_{Te} + 2V'''_{Sb} + (3/2)Te_2(g)\uparrow + 6h^{\cdot}$, where $h^{\cdot}$ denotes a produced hole and ↑ denotes volatilization of Te.[7,15] An increased Sb-to-Bi ratio in $Bi_xSb_{2-x}Te_3$ will increase the Sb_{Te} defects, which results in enhancement of the carrier density and reduction of the electrical resistivity. It has been reported that atoms can diffuse in a conductor under high-density electric current stressing, which is known as electromigration. Sb atoms have a highly effective charge for electromigration (~140 e) and are susceptible to electromigration-induced atomic diffusion.[16,17] An increased Sb-to-Bi ratio in $Bi_xSb_{2-x}Te_3$ will also compensate for the loss of Sb_{Te} defects caused by electromigration-induced atomic diffusion during the SPS process.

Figure 5 shows the temperature dependence of the Seebeck coefficient for sintered bulk $Bi_xSb_{2-x}Te_3$ + 0.1 vol.% SiC (x = 0.2, 0.25, 0.3, 0.34, 0.38, 0.42, 0.46, and 0.5) materials. The positive Seebeck coefficients indicate that all the samples are p-type. The Seebeck coefficient decreases with decreasing x value at low temperatures, and the maximum Seebeck coefficient at 323 K is reduced from 256 μV/K (x = 0.5) to 150 μV/K (x = 0.2), which is attributed to the enhanced carrier density. As the measurement temperature increases, the Seebeck coefficient decreases for x = 0.5, while it increases for x values lower than 0.3; for the latter, the maximum value is obtained at 473 K. When the x value is between 0.3 and 0.42, the Seebeck coefficient initially increases and then decreases, and the maximum value is obtained at 423 K. This phenomenon is mainly caused by the increase of carrier concentration with increasing Sb-to-Bi ratio, consequently the transition from extrinsic to intrinsic conduction is shifted to higher temperatures.[5]

Figure 6 shows the temperature dependence of the power factor for sintered bulk $Bi_xSb_{2-x}Te_3$ + 0.1 vol.% SiC (x = 0.2, 0.25, 0.3, 0.34, 0.38, 0.42, 0.46, and 0.5) materials. The power factors of all the samples show a maximum value near room temperature and then a decrease with increasing temperature. Although both electrical resistivity and Seebeck coefficient decrease with increasing Sb-to-Bi ratio, the power factor is still enhanced,

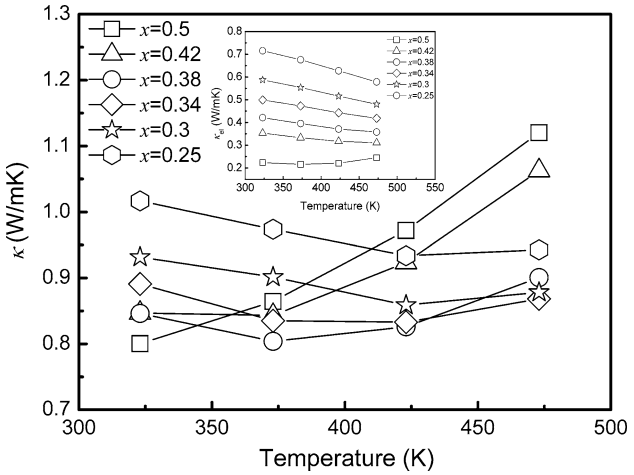

Fig. 7. Thermal conductivity of sintered bulk $Bi_xSb_{2-x}Te_3$ + 0.1 vol.% SiC (x = 0.25, 0.3, 0.34, 0.38, 0.42, and 0.5) materials as a function of measurement temperature.

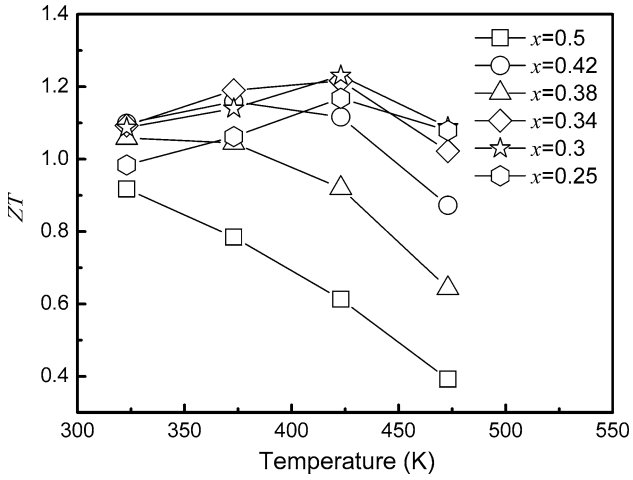

Fig. 8. Dimensionless ZT value of sintered bulk $Bi_xSb_{2-x}Te_3$ + 0.1 vol.% SiC (x = 0.25, 0.3, 0.34, 0.38, 0.42, and 0.5) materials as a function of measurement temperature.

since the decrease of electrical resistivity plays a dominant role in α^2/ρ, reaching a maximum value (3.14 mW/mK^2) at 323 K for $Bi_{0.3}Sb_{1.7}Te_3$, which is a great improvement over that (2.27 mW/mK^2) for $Bi_{0.5}Sb_{1.5}Te_3$. At x values below 0.3, the power factor at 323 K begins to decrease and drops to 2.94 mW/mK^2 for $Bi_{0.2}Sb_{1.8}Te_3$, which means that the decrease of the Seebeck coefficient plays a dominant role in α^2/ρ instead of the electrical resistivity.

Figure 7 shows the temperature dependence of the thermal conductivity for sintered bulk $Bi_xSb_{2-x}Te_3$ + 0.1 vol.% SiC (x = 0.25, 0.3, 0.34, 0.38, 0.42, and 0.5) materials. The thermal conductivity of $Bi_{0.5}Sb_{1.5}Te_3$ increases with temperature and reaches a minimum (0.8 W/mK) at 323 K. The increment of thermal conductivity at high temperatures might be attributed to bipolar diffusion arising from diffusion of electron–hole pairs with the onset of intrinsic excitation. The thermal conductivity of $Bi_xSb_{2-x}Te_3$ decreases slightly with increasing temperature between 323 K and 373 K for x values between 0.38 and 0.42, and decreases slightly with increasing temperature between 323 K and 423 K for x values between 0.25 and 0.34. This is because the increase of the Sb-to-Bi ratio can affect both the band gap structure and lattice phonon scattering. The thermal conductivity increases with decreasing x value at 323 K, which is attributed to the enhanced electronic thermal conductivity caused by the reduced electrical resistivity. The temperature dependence of the electronic thermal conductivity for different x values is shown in the inset to Fig. 7, which is according to the Wiedemann–Franz law ($\kappa_{el} = LT/\rho$, where L, T, and ρ are the Lorenz number, the temperature, and the electrical resistivity, respectively). When the temperature is above 373 K, the thermal conductivity decreases firstly when x is less than 0.38, but increases for x above 0.38, due to the change of electronic thermal conductivity and bipolar diffusion.[12] It has been reported that the increased carrier density not only reduces the electrical resistivity but also reduces the bipolar contribution to the electronic thermal conductivity at high temperatures and further reduces the bipolar thermal conductivity.[18]

Figure 8 shows the temperature dependence of the dimensionless ZT value for sintered bulk $Bi_xSb_{2-x}Te_3$ + 0.1 vol.% SiC (x = 0.25, 0.3, 0.34, 0.38, 0.42, and 0.5) materials. The samples with x between 0.3 and 0.38 show high ZT values of about 1.1 near room temperature. The maximum ZT value is about 1.23 at 423 K for $Bi_{0.3}Sb_{1.7}Te_3$. Both $Bi_{0.34}Sb_{1.66}Te_3$ and $Bi_{0.3}Sb_{1.7}Te_3$ show ZT values above 1.0 in the temperature range from 323 K to 473 K. The maximum ZT value of $Bi_{0.5}Sb_{1.5}Te_3$ with a commonly used Sb-to-Bi ratio is about 0.92 at 323 K and decreases markedly with increasing temperature. As compared with $Bi_{0.5}Sb_{1.5}Te_3$, the ZT value of $Bi_{0.3}Sb_{1.7}Te_3$ with a Sb-to-Bi ratio optimized for the present process shows a remarkable enhancement of about 17% at 323 K, and an even greater improvement has been achieved at higher temperature, which is attributed to the better power factor and relatively lower thermal conductivity at higher temperatures.

CONCLUSIONS

p-Type $Bi_xSb_{2-x}Te_3$ alloys with different Sb-to-Bi ratios were fabricated by MA and SPS. Both the electrical resistivity and Seebeck coefficient decreased with increasing Sb-to-Bi ratio. The maximum power factor value of 3.14×10^{-3} W/mK^2 was obtained for $Bi_{0.3}Sb_{1.7}Te_3$. Although this composition shows higher thermal conductivity at low temperatures, its value decreases with increasing temperature. As a result, higher ZT values are obtained for $Bi_{0.3}Sb_{1.7}Te_3$, with a maximum ZT value of 1.23 at 423 K, which is about twice that

(about 0.6) of $Bi_{0.5}Sb_{1.5}Te_3$ at the same temperature. The present study revealed that the optimal Sb-to-Bi ratio for the present process combining MA and SPS is different from that in the well-known composition $Bi_{0.5}Sb_{1.5}Te_3$. The maximum ZT value, 1.23 at 423 K, in the present nano-SiC-dispersed $Bi_{0.3}Sb_{1.7}Te_3$ materials is quite attractive for commercial applications such as cooling and low-temperature waste heat recovery applications.

ACKNOWLEDGEMENT

This work was supported by the National Basic Research Program of China (Grant No. 2007CB 607500) and National Nature Science Foundation (Grant No. 50820145203).

REFERENCES

1. L.E. Bell, *Science* 321, 1457 (2008).
2. B. Poudel, Q. Hao, Y. Ma, Y.C. Lan, A. Minnich, B. Yu, X. Yan, D.Z. Wang, A. Muto, D. Vashaee, X.Y. Chen, J.M. Liu, M.S. Dresselhaus, G. Chen, and Z. Ren, *Science* 320, 634 (2008).
3. J.R. Sootsman, D.Y. Chung, and M.G. Kanatzidis, *Angew. Chem. Int. Ed.* 48, 8616 (2009).
4. G. Chen, M.S. Dresselhaus, G. Dresselhaus, J.P. Fleurial, and T. Caillat, *Int. Mater. Rev.* 48, 45 (2003).
5. D.M. Rowe, *Thermoelectrics Handbook* (Boca Raton: CRC Press, 2006).
6. L.D. Zhao, B.P. Zhang, J.F. Li, H.L. Zhang, and W.S. Liu, *Solid State Sci.* 10, 651 (2008).
7. T.S. Oh, D.B. Hyun, and N.V. Kolomoets, *Scripta Mater.* 42, 849 (2000).
8. S.S. Kim, S. Yamamoto, and T. Aizawa, *J. Alloys Compd.* 375, 107 (2004).
9. W.J. Xie, X.F. Tang, Y.G. Yan, Q.J. Zhang, and T.M. Tritt, *J. Appl. Phys.* 105, 113713 (2009).
10. Y.Q. Cao, T.J. Zhu, X.B. Zhao, X.B. Zhang, and J.P. Tu, *Appl. Phys. A* 92, 321 (2008).
11. D. Lee, C. Lim, D. Cho, Y. Lee, and C. Lee, *J. Electron. Mater.* 35, 360 (2006).
12. L.D. Zhao, B.P. Zhang, J.F. Li, M. Zhou, W.S. Liu, and J. Liu, *J. Alloys Compd.* 455, 259 (2008).
13. L.D. Zhao, B.P. Zhang, J.F. Li, M. Zhou, and W.S. Liu, *Physica B* 400, 11 (2007).
14. J.F. Li and J. Liu, *Phys. Status Solidi A* 203, 3768 (2006).
15. L.D. Zhao, B.P. Zhang, W.S. Liu, H.L. Zhang, and J.F. Li, *J. Alloys Compd.* 467, 91 (2009).
16. C.N. Liao and L.C. Wu, *Appl. Phys. Lett.* 95, 052112 (2009).
17. C.N. Liao, L.C. Wu, and J.S. Lee, *J. Alloys Compd.* 490, 468 (2010).
18. Y.C. Lan, B. Poudel, Y. Ma, D.Z. Wang, M.S. Dresselhaus, G. Chen, and Z.F. Ren, *Nano Lett.* 9, 1419 (2009).